



QUANTITATIVE ANALYSIS OF THE DENDRITIC MORPHOLOGY OF CORTICOCORTICAL PROJECTION NEURONS IN THE MACAQUE MONKEY ASSOCIATION CORTEX

H. DUAN,^{a,b} S. L. WEARNE,^{b,c,d} J. H. MORRISON^{a,b,d,e} and P. R. HOF^{a,b,d,e,f*}

^aKastor Neurobiology of Aging Laboratories and Fishberg Research Center for Neurobiology,
Mount Sinai School of Medicine, New York, NY 10029, USA

^bComputational Neurobiology and Imaging Center, Mount Sinai School of Medicine, New York, NY 10029, USA

^cDepartment of Biomathematical Sciences, Mount Sinai School of Medicine, New York, NY 10029, USA

^dAdvanced Imaging Program, Mount Sinai School of Medicine, New York, NY 10029, USA

^eDepartment of Geriatrics and Adult Development, Mount Sinai School of Medicine, New York, NY 10029, USA

^fDepartment of Ophthalmology, Mount Sinai School of Medicine, New York, NY 10029, USA

Abstract—The polymodal association areas of the primate cerebral cortex are heavily interconnected and play a crucial role in cognition. Area 46 of the prefrontal cortex in non-human primates receives direct inputs from several association areas, among them the cortical regions lining the superior temporal sulcus. We examined whether projection neurons providing such a corticocortical projection differ in their dendritic morphology from pyramidal neurons projecting locally within area 46. Specific sets of corticocortical projection neurons were identified by *in vivo* retrograde transport in young macaque monkeys. Full dendritic arbors of retrogradely labeled neurons were visualized in brain slices by targeted intracellular injection of Lucifer Yellow, and reconstructed three-dimensionally using computer-assisted morphometry. Total dendritic length, numbers of segments, numbers of spines, and spine density were analyzed in layer III pyramidal neurons forming long projections (from the superior temporal cortex to prefrontal area 46), as well as local projections (within area 46). Sholl analysis was also used to compare the complexity of these two groups of neurons.

Our results demonstrate that long corticocortical projection neurons connecting the temporal and prefrontal cortex have longer, more complex dendritic arbors and more spines than pyramidal neurons projecting locally within area 46. The more complex dendritic arborization of such neurons is likely linked to their participation in cortical networks that require extensive convergence of multiple afferents at the cellular level. © 2002 IBRO. Published by Elsevier Science Ltd. All rights reserved.

Key words: cognition, dendrites, intracellular injection, primate neocortex, pyramidal neurons, spines.

Cognitive functions in mammals are likely to rely on the activity of large-scale networks of functionally interconnected cortical regions (Bressler, 1995; Mesulam, 1998; Compte et al., 2000). Such networks are subserved by long-range corticocortical pathways that link multiple association areas in the cerebral cortex, such that a given polymodal association area (e.g. cortical regions in the superior temporal gyrus or in the dorsolateral prefrontal cortex) receives numerous convergent inputs from other association cortices. For example, the association areas in the parietal, temporal, and parahippocampal cortex are reciprocally linked with each other as well

as with the prefrontal cortex through long association corticocortical pathways (for reviews, see Goldman-Rakic, 1988, 1995, 1996; Barbas, 1992; Weinberger, 1993), providing an anatomical substrate for certain cognitive functions (Bressler, 1995; Mesulam, 1998; Compte et al., 2000). Layer III pyramidal neurons are the major cell type furnishing these long association corticocortical pathways (Jones, 1984; Barbas, 1986; de Lima et al., 1990; Campbell et al., 1991; Hof et al., 1995). Interestingly, the cortical neurons forming long corticocortical pathways are thought to be particularly vulnerable in Alzheimer's disease (Morrison et al., 1987; Hof and Morrison, 1990; Hof et al., 1990), further supporting the notion that these neurons are crucial mediators of cognitive and memory functions in primates (Hof et al., 1990; Morrison, 1993; Morrison and Hof, 1997). In addition, we have demonstrated that the neurons furnishing long corticocortical connections between association cortices differ in their neurochemical phenotype from those providing short projections and their vulnerability is partially dependent on their particular neurochemical attributes (Hof et al., 1995, 2002).

*Correspondence to: P.R. Hof, Kastor Neurobiology of Aging Laboratories, Box 1639, Mount Sinai School of Medicine, One Gustave L. Levy Place, New York, NY 10029, USA. Tel.: +1-212-659-5904; fax: +1-212-849-2510.

E-mail address: patrick.hof@mssm.edu (P. R. Hof).

Abbreviations: FB, Fast Blue; LY, Lucifer Yellow; PBS, phosphate-buffered saline.

Recent studies in macaque monkeys have demonstrated the existence of local horizontal connections between groups of pyramidal cells within the prefrontal cortex (Levitt et al., 1993; Lund et al., 1993; Kritzer and Goldman-Rakic, 1995; Pucak et al., 1996; Melchitzky et al., 1998). The axons of pyramidal cells in layers II and III of the prefrontal cortex extend horizontally for some distance (up to 7–8 mm) and form discrete, stripe-like clusters of axon terminals in cortical layers I to III (Levitt et al., 1993; Pucak et al., 1996). These axon terminals form exclusively asymmetric synapses and contact primarily the dendritic spines of other excitatory neurons, presumably pyramidal neurons (Melchitzky et al., 1998). A double-labeling study also suggested that the intrinsic horizontal connections in the prefrontal cortex are reciprocal (Pucak et al., 1996). This pattern of connections has been implicated as a functional substrate for reverberating excitatory circuits amongst primate association cortices (Pucak et al., 1996; Melchitzky et al., 1998), which are known to be involved in working memory in the prefrontal cortex (Goldman-Rakic, 1988, 1995, 1996), and as such are less likely to mediate the long distance inter-regional communication with other association areas.

Although much is known about the topographic distribution, cell typology, and organization of the axon terminals of many corticocortical projection neurons, little effort to date has been expended to define the detailed dendritic morphology of specific types of cortical neurons giving rise to corticocortical projections in association cortex (de Lima et al., 1990; Nimchinsky et al., 1996; Duan et al., 2000; Soloway et al., 2002). A few studies in rat and cat suggested that cortical pyramidal cells in the same layer of the infragranular layers have distinct morphological features related to their projections (Katz, 1987; Hallman et al., 1988; Hübener and Bolz, 1988; Hübener et al., 1990; Kasper et al., 1994; Rumberger et al., 1998). Only one study in the cat has related the morphological features of pyramidal cells to their projection types in the superficial layers of the visual cortex (Matsubara et al., 1996). However, so far there is only limited evidence whether pyramidal cells in the association cortex that give rise to a particular type of corticocortical projection have a distinct dendritic architecture that might render them recognizably different from those giving rise to another type of corticocortical projection (Duan et al., 2000; Soloway et al., 2002). In addition, recent studies in human and non-human primates have described a hierarchical increase in the size, complexity, and spine density of basal dendritic field of cortical layer III pyramidal neurons from primary cortices to unimodal and polymodal association areas (Elston et al., 1996, 1999a–c, 2001; Elston and Rosa, 1997, 1998; Jacobs et al., 1997, 2001; Elston, 2000).

We predicted that the complexity of the neurons providing the convergent corticocortical circuits interconnecting areas such as area 46 and the superior temporal cortex would be reflected at the cellular level, in that these neurons should have highly complex dendritic trees with high numbers of spines to accommodate

the regional convergence on a cellular level. To test this hypothesis, we quantified and compared several morphometric parameters of the dendritic arbor in neurons projecting from the superior temporal cortex to area 46 with pyramidal neurons that project locally within area 46.

EXPERIMENTAL PROCEDURES

Animals and surgical procedures

Five adult male long-tailed macaque monkeys (*Macaca fascicularis*; 10–12 years old) were used in this study. All experimental protocols were conducted according to National Institutes of Health (NIH) guidelines for animal research and were approved by the Institutional Animal Care and Use Committee at Mount Sinai School of Medicine. The animals were tranquilized with ketamine hydrochloride (25–25 mg/kg i.m.), intubated, and maintained under isoflurane general anesthesia and strict sterile surgical conditions. They were placed for surgery in a custom-designed large animal head holder (David Kopf Instruments, Tujunga, CA) and a craniotomy was performed over the cortical site. The animals received injections of the retrograde tracer Fast Blue (FB) in ventral area 46 (Fig. 1). An aqueous solution of FB (4%; Sigma, St. Louis, MO, USA) was injected into the left hemisphere using a 5- μ l Hamilton microsyringe with a 24-gauge needle. Injections were placed at depths from 0.6 to 1.2 mm below the pial surface. Nine to 12 300–400 nl injections were placed in each animal and none penetrated the underlying white matter. Following surgery, a survival time of 21 days was set to allow for optimal retrograde transport. Then the animals were perfused intracardially as previously described (Hof et al., 1995; Nimchinsky et al., 1996). In brief, the animals were deeply anesthetized with ketamine hydrochloride (25 mg/kg) and pentobarbital sodium (20–35 mg/kg i.v.), intubated, and mechanically ventilated. The chest was opened to expose the heart, and 1.5 ml of 0.1% sodium nitrite was injected into the left ventricle. The descending aorta was clamped and the monkeys were perfused transcardially with cold 1% paraformaldehyde in phosphate-buffered saline (PBS) for 1 min, and then for 12 min with cold 4% paraformaldehyde and 0.125% glutaraldehyde in PBS.

Tissue preparation

Following perfusion, the brain was removed from the skull and 4–5-mm-thick slabs of tissue were obtained from the prefrontal and temporal cortex. These tissues were blocked in a plane perpendicular to the principal sulcus in the prefrontal cortex or to the superior temporal sulcus in the temporal cortex. Blocks of tissue containing the injection sites and region adjacent to them in the rostral or caudal directions within area 46 were dissected out from the brain. The blocks containing the injection sites were used for Nissl staining to verify the injections. These blocks were postfixed for 6 h in the same fixative, sectioned at 40 μ m on a Vibratome and stained with Cresyl Violet. One block of tissue adjacent to the injection sites was used for intracellular injection. FB-labeled cells in this area form local intrinsic horizontal corticocortical projections (for simplicity, called local projections hereafter) within area 46 (Pucak et al., 1996; Melchitzky et al., 1998). Another block of tissue used for cell loading was taken from the cortex located in the fundus of the superior temporal sulcus, corresponding to areas TPOr, IPa and TEa (de Lima et al., 1990; Cusick et al., 1995). In our experiment, the FB-labeled cells visualized in this area formed long association corticocortical projections (hereafter referred to as long projections) from the temporal cortex to area 46 (de Lima et al., 1990; Hof et al., 1995). These blocks were postfixed for 2 h in the same fixative. Then they were placed into PBS and cut at 400 μ m on a Vibratome. Sections were cut in a plane perpendicular to the pial surface.

Intracellular injections

For intracellular injection, the sections were mounted on nitrocellulose filter paper and immersed in PBS. FB retrogradely labeled pyramidal cells in the supragranular layers were identified under epifluorescence with a UV filter, impaled with sharp micropipettes, and loaded with 5% Lucifer Yellow (LY; Molecular Probes, Eugene, OR, USA) in dH₂O under a DC current of 3–8 nA for 10–12 min, or until the dye had filled distal processes and no further loading was observed (de Lima et al., 1990; Nimchinsky et al., 1996). Generally, three to four cells were injected per slice, and injections were far enough apart to avoid overlapping of the dendritic trees. After neuronal labeling, sections were fixed again in 4% paraformaldehyde and 0.125% glutaraldehyde in PBS for 4 h at 4°C, washed, and stored in PBS. In order to be included for three-dimensional reconstruction and further analysis, filled neurons had to satisfy four criteria: (1) they had to be located in layer III. Accurate determination of cortical layers was performed on the fixed slice after counterstaining selected sections with 4,6-diamidino-2-phenylindole (Sigma), which is a fluorescent nucleic acid stain; (2) the dendritic tree of the pyramidal cell had to be filled completely, which was judged by tracing higher order branches to abrupt, well-defined tips (Nimchinsky et al., 1996; Elston and Rosa, 1997, 1998); (3) the soma–apical dendrite orientation had to be perpendicular to the pial surface; and (4) absence of adjacent cells filled by the same injection and a reasonable distance between individual cells had to allow for unambiguous determination of the exact origin of every dendritic segment.

Quantitative analyses

Sections containing selected LY-filled neurons were then coverslipped with PermaFluor mounting medium and reconstructed using a computer-assisted morphometry system, consisting of a Zeiss Axiophot photomicroscope equipped with a Zeiss MSP65 computer-controlled motorized stage, a Zeiss ZVS-47E video camera system, a Macintosh G3 computer, and custom-designed morphometry software NeuroZoom (Nimchinsky et al., 1996; Young et al., 1997; Hof et al., 2000). This system allows for accurate mapping and tracing of the cell processes in all three dimensions. Neurons were visualized first using a Zeiss Fluor 10× objective, and their locations within the tissue sections were mapped (Fig. 1A–D). Then the loaded neurons were drawn using a Zeiss Apochromat 100× objective with a numerical aperture of 1.4. A live RGB image was ported to the computer screen and mapping was performed by moving the stage in 1-μm steps through the z-axis along the length of each dendrite. Spines were plotted at the same time. Then, the section itself was drawn at 10×. In this manner, the x, y, and z coordinates of each dendritic segment and spine were recorded to enable later three-dimensional representation and rotation of the reconstructed neuron (Nimchinsky et al., 1996). Three to eight cells were reconstructed from each type of projection neurons for each subject. The NeuroZoom datasets were then exported to generate three-dimensional renderings of the traced neurons using NeuroGL, a self-contained, compact, and fast application to visualize structural details of neurons, including branching patterns, spine location, and spine density, at a range of scales and in an interactive three-dimensional environment (Rodriguez et al., 2001).

Dendrograms showing the branching pattern of each dendritic tree were prepared for each neuron. By using the three-dimensional capabilities of the software, we quantified the following parameters for each cell: 1) total dendritic length, representing the summed length of dendritic segments; 2) dendritic segment counts, representing the total number of dendritic segments; 3) total dendritic spine number, representing the sum of all spines on dendritic segments; and 4) dendritic spine density, representing the average number of spines per μm of dendritic length. In addition, the dendritic branching patterns were analyzed using Sholl's method (Sholl, 1953). The number of den-

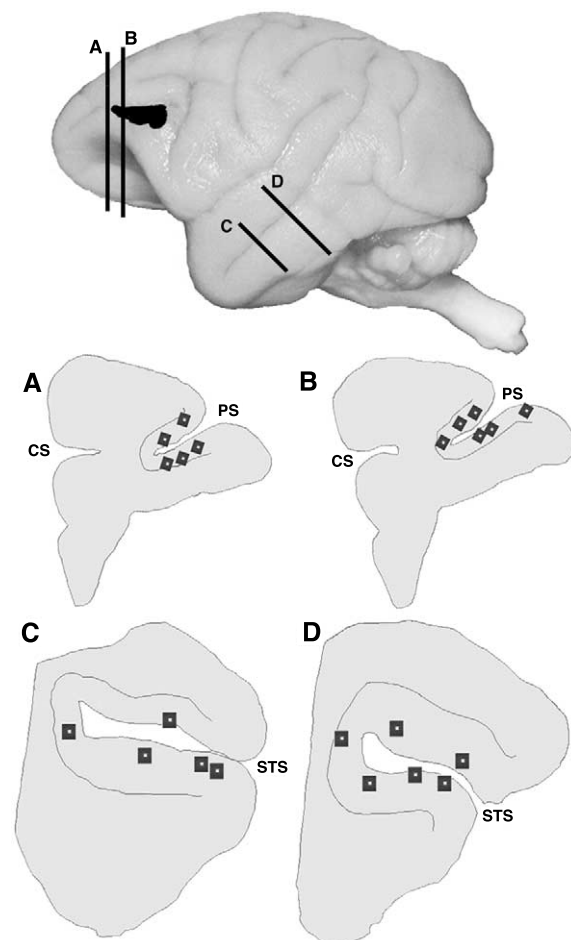


Fig. 1. Surface rendering of the lateral view of a macaque monkey (*Macaca fascicularis*) brain, showing the maximal extension of the intracortical FB injections obtained from series of Nissl-stained sections (black area) in area 46 of five macaque monkeys. The maps A–D illustrate representative sections in which retrogradely labeled neurons were filled with LY and reconstructed. The location of the sections is indicated on the view of the brain above. Each section was traced at 10× magnification, and the localization of the LY-filled neurons plotted (light dots on black boxes). These boxes actually correspond to screen dumps from the computer software that are embedded in the low power maps. CS, cingulate sulcus; PS, principal sulcus; STS, superior temporal sulcus.

dritic intersections crossing each 20-μm radius ring progressively more distal from the soma was counted.

Statistical testing was performed using analysis of variance to assess possible differences in the various morphometric parameters among cases for both neuronal types. As the variance between was smaller than that within animals and the variances of each subject did not significantly differ for each of the measured parameters, data were expressed as means from all the animals for both groups of neurons. Projection type-specific differences in these variables across the total, apical, and basal dendritic domains were then assessed by comparing means using Tukey tests for groups with unequal numbers. Finally the data from the Sholl analyses were also expressed as cumulative frequencies and statistical differences between the two neuronal populations were assessed using the Kolmogorov–Smirnov test. Differences were considered statistically significant at $P < 0.05$.

RESULTS

Morphology of the LY-filled neurons

The injections of FB in the ventral part of area 46 resulted in comparable numbers of retrogradely labeled local projection neurons within area 46 and the long projection neurons in the cortex lining the superior temporal sulcus. The local projection neurons were located primarily in layer II and layer III, which is consistent with previous studies in macaque monkey prefrontal cortex (Kritzer and Goldman-Rakic, 1995; Pucak et al., 1996; Melchitzky et al., 1998). The long projection neurons formed two clearly defined bands, corresponding to layer III, and layers V and VI. This pattern of laminar distribution for long projection neurons is in agreement

with earlier macaque monkey studies (de Lima et al., 1990; Hof et al., 1995).

Forty-eight local projection neurons and 55 long projection neurons in layer III were intracellularly injected with LY. Of these, 46 neurons (27 long projection neurons and 19 local projection neurons) were reconstructed (Duan et al., 2000). All of the filled neurons used for quantitative analysis exhibited a typical pyramidal morphology with extensive dendritic branching and large numbers of spines (Figs. 2, 3).

Quantitative analysis of dendrites

There were no differences in morphometric parameters among the animals within each group of projection neurons, and therefore data from each projection type were

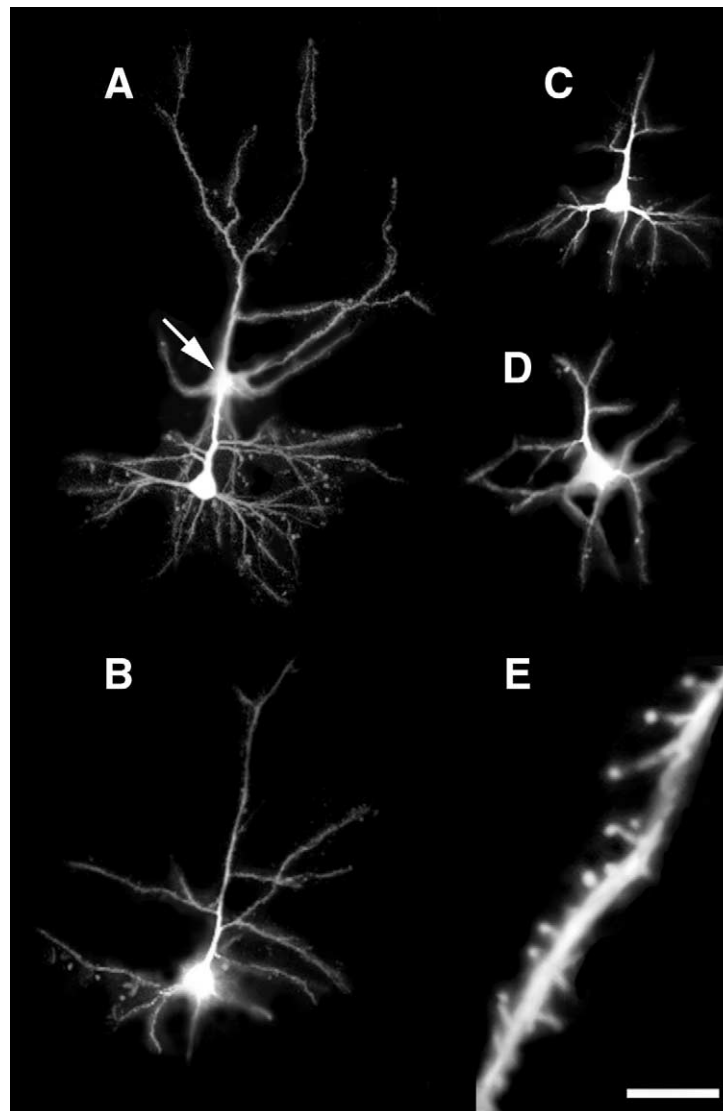


Fig. 2. Examples of LY-filled long projection neurons (A, B) and short projection neurons (C, D). The neuron in A was filled from its apical dendrite (the arrow shows the site of injection). Note the more extensive dendritic arbors of the long projection neurons. Panel E shows a high power photomicrograph of a segment of an apical dendrite of a layer III pyramidal neuron injected with Lucifer Yellow. Note the high quality of the LY filling, permitting optimal tracing and mapping of the spines. Scale bar (on E) = 50 μ m (A–D) and 5 μ m (E).

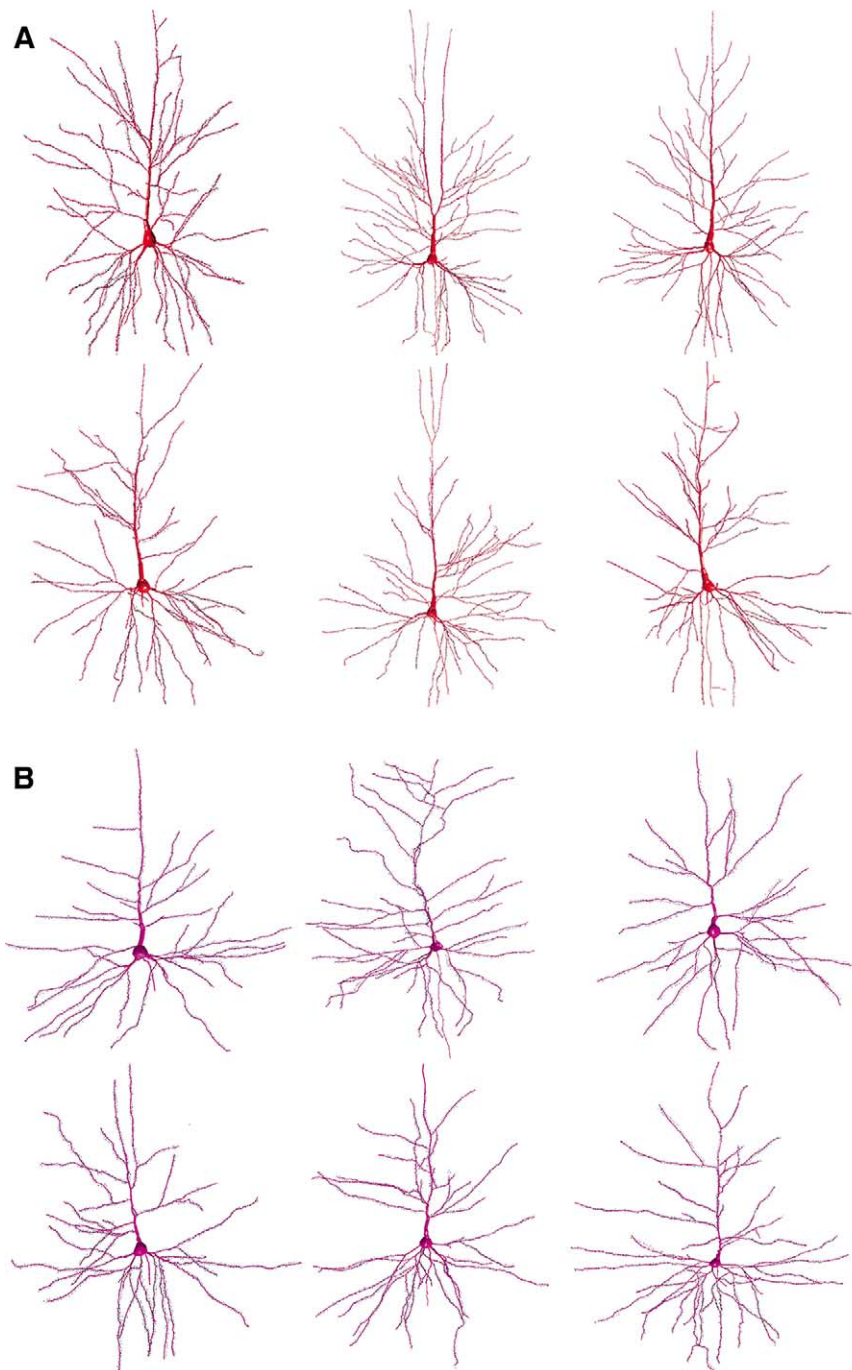


Fig. 3. Representative examples of three-dimensional reconstructions of corticocortically projecting pyramidal cells with the spines (blue dots) plotted onto the dendritic trees (in red). These three-dimensional reconstructions of neurons were obtained using NeuroGL and are rendered with variable scaling and degrees of rotation about their principal axis to depict the extent of their basal and apical dendritic arborization. Neurons in A are long projection neurons and neurons in B are local projection neurons. Note that the long projection neurons shown in A exhibit an apparently more complex dendritic structure than the local projection neurons depicted in B.

pooled across animals. Examples of reconstructed neurons forming long projections and local projections are shown in Fig. 3. Quantitative measures revealed a significant difference between projection types for both the dendritic length and apparent complexity (Table 1 and Fig. 4). Long projection neurons had longer dendritic lengths ($P < 0.05$) and more dendritic segments ($P < 0.01$) than local projection neurons in their apical

dendrites. Statistically significant differences between projection types were also observed in the basal dendrites for both dendritic length ($P < 0.05$) and dendritic segment numbers ($P < 0.01$). The total length of the dendrites was longer in long projection neurons ($P < 0.05$), and these cells also had overall more dendritic segments ($P < 0.05$).

Furthermore, long projection neurons had higher

Table 1. Morphometric analysis of cortical neurons forming long and local projections

Parameter	Long (n = 27)	Short (n = 19)	% Difference	P Value
<i>Total dendritic length</i>				
Total	5517.4 ± 247.0	4138.7 ± 218.9	-25.0	< 0.05
Apical	2553.8 ± 194.5	1870.5 ± 156.4	-26.8	< 0.05
Basal	2963.6 ± 112.6	2268.2 ± 109.2	-23.5	< 0.05
<i>Total dendritic segments</i>				
Total	86.9 ± 3.2	63.8 ± 2.9	-26.6	< 0.01
Apical	35.3 ± 2.3	26.0 ± 1.8	-26.4	< 0.01
Basal	51.7 ± 1.8	37.8 ± 2.0	-26.8	< 0.01
<i>Total spine number</i>				
Total	2799.5 ± 122.2	2328.3 ± 187.0	-16.8	< 0.05
Apical	1356.4 ± 102.9	1118.5 ± 118.1	-17.5	n.s.
Basal	1443.0 ± 55.7	1209.8 ± 82.4	-16.2	< 0.05
<i>Spine density</i>				
Total	0.51 ± 0.01	0.55 ± 0.02	+7.8	n.s.
Apical	0.54 ± 0.01	0.58 ± 0.03	+7.4	n.s.
Basal	0.49 ± 0.01	0.53 ± 0.02	+8.2	n.s.

Dendritic lengths are in μm and spine densities are expressed per μm of dendrite. Data represent means \pm S.E.M. Note that the differences between long and local projection neurons are about dendritic complexity and spine numbers, but that the spine densities are not different between the two groups of investigated neurons. n.s., non-significant.

spine numbers than local projection neurons on their basal dendrites ($P < 0.05$; Fig. 4). In contrast, there was no statistically significant difference in spine numbers for the apical dendrites and spine density for both apical and basal dendrites (Table 1). However, the fact that long projection neurons had more extensive dendritic arbors than short projection neurons and an apparent larger size overall suggest that the trend toward higher spine densities in short projection neurons shown in Table 1 may have a functional significance.

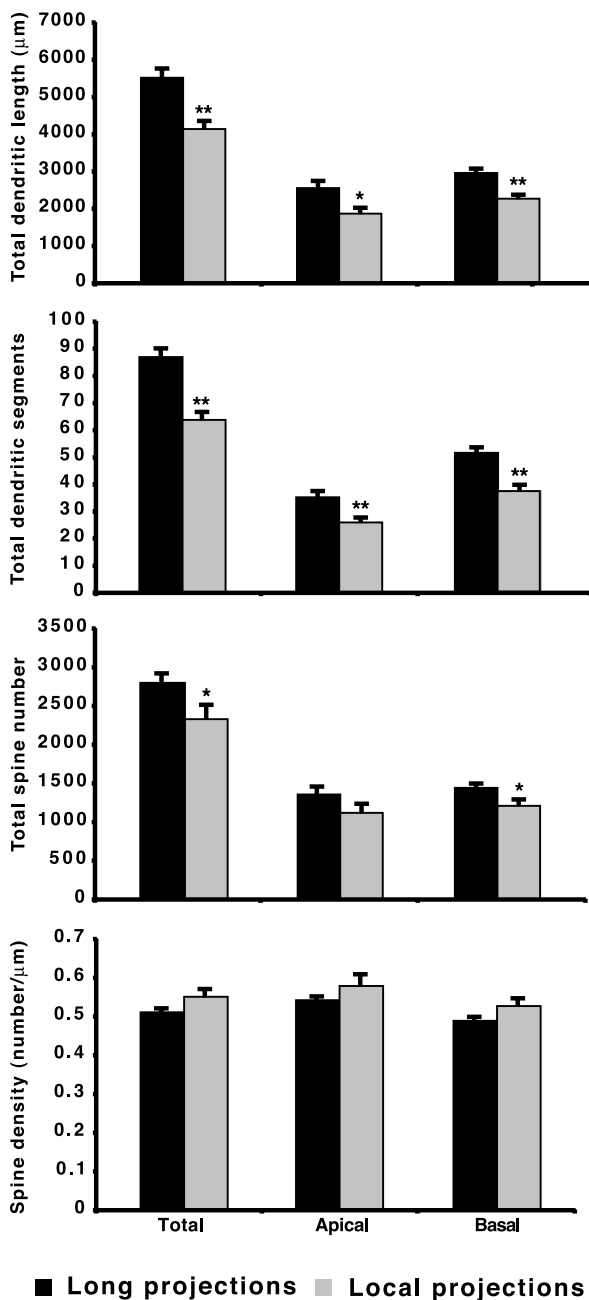
Dendrograms of representative neurons forming long projections and local projections are shown in Fig. 5. These dendrograms, obtained from the reconstruction of the cells with the NeuroZoom software, demonstrate the overall branching pattern of the dendritic trees and are scaled in terms of length and complexity. This analysis also revealed a qualitative difference between the two types of projections for the dendritic complexity of both the apical and basal dendrites (Fig. 5). The complexity of apical and basal dendritic trees for the two types of projection neurons was further assessed using Sholl analysis (Fig. 6). The maximal Sholl intersection radius of the apical dendritic tree for the local projection neurons was 440 μm , whereas it was 760 μm for the apical dendritic tree of the long projection neurons (Fig. 6). There were more intersections in the long projection neurons than local projection neurons after a radius of 80 μm , with a significant difference between radii 100 and 220 μm (Fig. 6). The maximal Sholl intersection radius of the basal dendritic tree for the local and long projection neurons was similar (280 and 300 μm , respectively; Fig. 6). However, when the entire dendritic tree was considered as a whole, there was a significant difference for all radii between 40 μm and 180 μm (Fig. 6; $P < 0.01$, except for the 40-, 180-, and 200- μm levels, where $P < 0.05$), with more bifurcations on the basal dendrites of the long projection neurons than on the local projection neurons. Finally, the distribution cumulative frequency of Sholl intersections along the dendritic arbors

was significantly different between the long and short projection neurons ($P < 0.002$ for total and apical arbors, and $P < 0.05$ for basal arbors; Fig. 6).

DISCUSSION

In this study, we examined the dendritic morphology of layer III pyramidal neurons forming local and long corticocortical projections in macaque monkey neocortex. By comparing the dendritic length, branching pattern, spine numbers, and spine density of layer III pyramidal cells that provide local (i.e. within area 46) and long (i.e. from the cortex lining the superior temporal sulcus to area 46) corticocortical projections, we found that distant neurons furnishing long projections to area 46 have larger and more complex dendritic arbors with a greater number of dendritic spines than resident neurons providing short intraregional projections. We have shown that these same two circuits differ in key neurochemical attributes (Hof et al., 1995, 2002). In addition, other studies have shown that cortical pyramidal cells have distinct morphological features that are related to the types of projection they provide (Katz, 1987; Hallman et al., 1988; Hübener and Bolz, 1988; Hübener et al., 1990; Kasper et al., 1994; Matsubara et al., 1996; Rumberger et al., 1998). These earlier morphological studies were conducted in the visual cortex of the rat and cat and mostly focussed on neurons in infragranular layers of visual cortex with different target areas. Our design differed from these studies in that the target region was similar (i.e. area 46), yet the origin differed (i.e. local area 46 neurons vs. distant superior temporal cortex neurons). Both designs revealed distinct morphological differences among pyramidal cells in the same layer of association cortex (i.e. layer III) that furnish fundamentally different connections.

The combination of *in vivo* tract-tracing and cell loading in fixed slices yields high-quality labeling of dendritic



■ Long projections ■ Local projections
 Fig. 4. Histograms showing the quantitative data for long and local projection neurons from the five macaque monkeys used in this study. Statistically significant differences are indicated by asterisks (* $P < 0.05$; ** $P < 0.01$). The bars represent means \pm S.E.M.

structures (dendrites and dendritic spines) of selected neurons (de Lima et al., 1990; Nimchinsky et al., 1996; Duan et al., 2000). This is critical for a quantitative analysis of dendritic extent and spine numbers on identified neurons. However, some practical problems do exist at present. As addressed elsewhere (Uylings et al., 1986; Jacobs et al., 1997), sectioning tissue at 400 μm will result in cut dendritic segments. Therefore, measurements in this study represent estimates rather than absolute values because the full dendritic extent may not be exactly assessed in all cases with certainty. It is likely that

there might be more cut segments for larger neurons forming long projections than smaller neurons forming local projections. Furthermore, with respect to spine measurements, spines that either lie on the backside of the dendrite or are pointing directly up at the viewer cannot be seen reliably with standard light microscopy (Trommald and Hulleberg, 1997). Thus measurements of spine density with the light microscope will necessarily underestimate the total number of spines. However, since this affects all neurons equally there is no direct effect on the differences of the spine density between the two types of projections. Thus the actual projection type differences in both dendritic and spine measurements may actually be larger than observed in the present study because of the possibility that more segments were cut in long projection neurons. We did not observe in the present study significant differences in spine densities across projection types, although we cannot exclude the possibility that regional constraints can affect arborization patterns

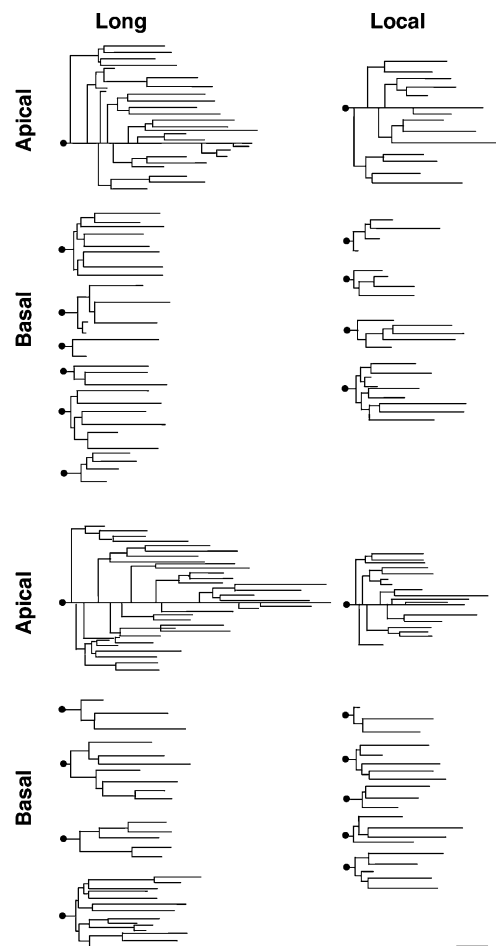


Fig. 5. Representative dendrograms of apical and basal dendritic trees of long and local projection neurons. The soma of these neurons would be located to the left of the dendrites (noted by a dot). The dendrogram shows the general branching patterns of the dendritic tree. It is also scaled in terms of length and complexity. The long projection neurons have an apparently more complex dendritic arborization than the local projection neurons. The basal dendrites are shown under the apical tree of the same neuron in each case. Scale bar = 50 μm .

Sholl Analysis

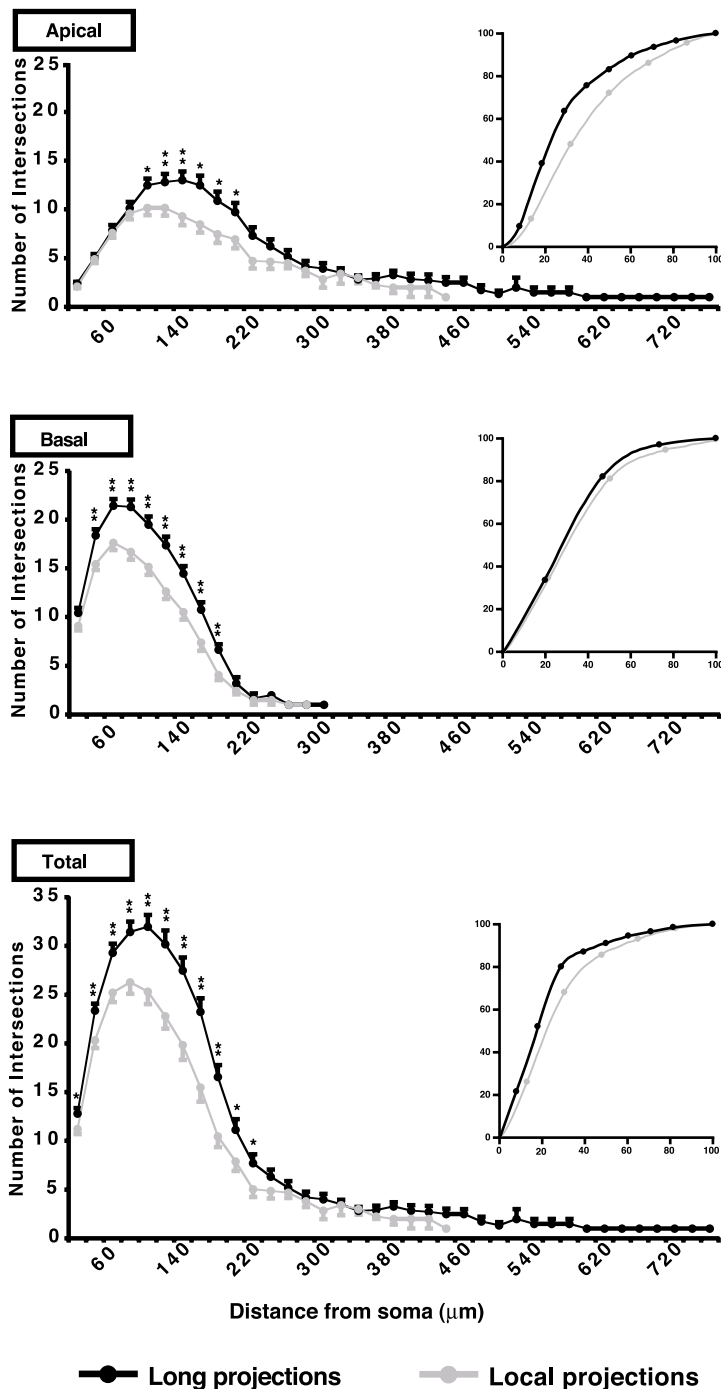


Fig. 6. Sholl analysis of long projection (dark) and local projection (gray) neurons in the five macaque monkeys. Asterisks indicate statistically significant differences across the dendritic trees ($*P < 0.05$; $**P < 0.01$). Values represent means \pm S.E.M. Cumulative frequency plots of the distribution of Sholl intersections along the dendritic trees also revealed statistically significant differences between long and local projection neurons (insets; $P < 0.002$ for apical and total arbors and $P < 0.05$ for basal arbors). The x and y axis values on the insets represent cumulative frequencies in % (for clarity, some of the data points were omitted).

and may be an influencing factor for the spine density measurements (Lund et al., 1993; Jacobs et al., 1997, 2001; Elston and Rosa, 1997, 1998; Elston et al., 1999a,b, 2001; Elston, 2000). In this context it should be noted that the neurons of origin of long projections

appear to be larger than locally projecting neurons (Hof et al., 1995) and have more elaborate dendritic trees (Fig. 2). It is thus possible that spines are actually denser in neurons from area 46 compared to neurons from the superior temporal cortex as suggested by the observed

trend. This may be functionally relevant in the context of the role of the prefrontal networks in working memory (Goldman-Rakic, 1995, 1996; Compte et al., 2000; Miller and Cohen, 2001), in that these short projection neurons are receiving convergent information from local networks (Pucak et al., 1996; Melchitzky et al., 1998), on a smaller dendritic tree.

Given the fact that prefrontal pyramidal neurons as a group show a significantly higher degree of branching than those in the temporal lobe (Elston, 2000; Elston et al., 2001; Jacobs et al., 2001), the observed projection type differences in the dendritic length and complexity reported here are particularly impressive, since the local projection neurons were chosen from the prefrontal region and the long projection neurons were sampled from the temporal cortex. In this respect, it should be noted that the prefrontal population of neurons investigated by Elston and colleagues (Elston, 2000; Elston et al., 2001) were sampled from a different region than in the present analysis, namely, in the frontopolar area 10. These authors also studied the inferior temporal cortex, and focussed on the basal dendrites (Elston et al., 1999a,b, 2001). Our data are, however, supported by a recent study (Henry et al., 2002) that used a mass-multifractal approach to quantify difference in neuronal morphology and showed significant differences in the global complexity of dendritic arborization between long and local projection neurons. Furthermore, it could be argued that the observed differences could be attributed to differences in the afferent connectivity of the two areas which in turn exhibit specific architectural and functional characteristics. In this study we focussed our analysis on neurons labeled from a local injection and neurons distant from that site, based on our previous data on macaque monkey corticocortical connectivity (Hof et al., 1995). We have preliminary evidence from a limited sample of neurons that the reciprocal projection from area 46 to the superior temporal cortex does not differ in the parameters analyzed here from the neurons projecting from the temporal to the prefrontal cortex. Clearly, future analyses of pyramidal cell morphology comparing neurons of similar regional origin with different target regions will be instructive.

One of the most significant structural features of the neurons in the central nervous system is the potentially large synaptic surface they attain by the extension of their dendritic processes. Sholl (1955) estimated that dendrites form 90–95% of the receptive surface of the neurons in the cat sensorimotor and visual cortices. The dendrites and spines of pyramidal cells are postsynaptic sites for both excitatory and inhibitory inputs (DeFelipe and Fariñas, 1992; Somogyi et al., 1998). Therefore, differences in the length and complexities in the dendritic arbors of cortical pyramidal cells reflect the putative differences in the number of excitatory and inhibitory inputs received by individual neurons (Jacobs et al., 1997, 2001; Elston and Rosa, 1997, 1998; Elston et al., 1999a,b, 2001; Elston, 2000). Thus, pyramidal cells forming the long projections with more complex dendritic trees and more spines are likely to be able to integrate a larger number of inputs, which is required to

perform complex cortical functions that underlie cognition (Bressler, 1995; Hof et al., 1995; Yuste and Tank, 1996; Mesulam, 1998; Miller and Cohen, 2001; Nimchinsky et al., 2002). In contrast, the apparently more limited dendritic arborizations of the local projection neurons in the prefrontal cortex may be a reflection of the fact that these neurons are predominantly the targets of the intrinsic axonal patches (Lund et al., 1993; Pucak et al., 1996; Melchitzky et al., 1998) that enable local processing rather than extensive inter-regional convergence. We cannot in the present study ascertain that our local projection neurons do not furnish some association projections to neighboring cortical areas within the prefrontal cortex. Evidence for this type of dual projections has been documented in detail in double-labeling studies combined with electron microscopy that showed very similar numbers of asymmetric synapses, nearly all of them on spines, formed by axons traced from either local injection sites or through some distance in the prefrontal cortex, indicating that the same neurons can furnish both types of connections (Pucak et al., 1996; Melchitzky et al., 1998).

The morphologic differences between the two circuits analyzed here are accompanied by other cellular specializations that are reflected in neurochemical phenotype. Other analyses (Hof et al., 1995, 2002) have shown that the neurons furnishing the superior temporal cortex to area 46 projection virtually all have a high abundance of neurofilament protein in the somatodendritic domain, whereas less than 25% of the neurons projecting within area 46 display this attribute. The correspondence with complex morphology described here suggests that the abundant somatodendritic neurofilament protein is required to support the dendritic arbor required for extensive convergence in these circuits (Hof et al., 1995). It is notable that this particular attribute may also render the homologous neurons vulnerable to degeneration in humans with Alzheimer's disease (Hof et al., 1990; Hof and Morrison, 1990; Morrison and Hof, 1997).

Although these data compare only two different circuits, they suggest that neurons furnishing long projections interconnecting polymodal association cortices will generally have more complex dendritic trees compared to pyramidal neurons that project locally. The present results agree and complement a recent study reporting that callosal projections to areas 9 and 46 of the macaque monkey prefrontal cortex have more extensive apical and basal arbors than local ipsilateral projections (Soloway et al., 2002). Interestingly, these authors found higher spine densities on their long (callosal) projection neurons, pointing to the possible existence of a range of spine distributions on corticocortical neurons which may have considerable functional repercussions. Clearly, the role played by corticocortically projecting neurons in the superior temporal gyrus and in area 46 in cognitive processing requires integration of inputs from a large number of other neocortical areas, parahippocampal areas, as well as thalamic nuclei. The present data suggest that the extensive convergence is reflected on a cellular level as well as a regional level,

in that the neurons providing connections from a distant, functionally linked region have dendritic arbors and spine numbers suitable for the reception of a large number of convergent inputs, implying that there is a system linking neurons with a high capacity for convergence, as one would expect. Such morphologic complexity subserving extensive convergence would be expected to be reflected in complex response properties (Yuste and Tank, 1996) for neurons in superior temporal or prefrontal cortex (Miller and Cohen, 2001). Should the dendritic arbor of these neurons be compromised, for example, during aging (Page et al., 2002; Nimchinsky et al., 2002), then their possible role in mediating cognition

would be compromised. Non-human primate studies are currently underway to test this hypothesis.

Acknowledgements—We thank Drs. E.A. Nimchinsky, P.R. Rapp and G.N. Elston for valuable discussion, Dr. Y. He, B. Wicinski, G. Volmar, and R. Jenkins for help with animal surgery and postoperative care, A. Rodriguez, K.T. Kelliher, R.A. Shah, and Dr. W.G. Young for software development, W.G.M. Janssen, S. Fink, and Dr. J.D. Hao for assistance with cell loading, and A.P. Leonard and T. Flores for help with graphics. This work was supported by NIH grants AG05138 and AG06647, by the Howard Hughes Medical Institute, and by the Mount Sinai School of Medicine.

REFERENCES

- Barbas, H., 1986. Pattern in the laminar origin of corticocortical connections. *J. Comp. Neurol.* 252, 415–422.
- Barbas, H., 1992. Architecture and cortical connections of the prefrontal cortex in the rhesus monkey. *Adv. Neurol.* 57, 91–115.
- Bressler, S.L., 1995. Large-scale cortical networks and cognition. *Brain Res. Rev.* 20, 288–304.
- Campbell, M.J., Hof, P.R., Morrison, J.H., 1991. A subpopulation of primate corticocortical neurons is distinguished by somatodendritic distribution of neurofilament protein. *Brain Res.* 539, 133–136.
- Compte, A., Brunel, N., Goldman-Rakic, P.S., Wang, X.I., 2000. Synaptic mechanisms and network dynamics underlying spatial working memory in a cortical network model. *Cereb. Cortex* 10, 910–923.
- Cusick, C.G., Seltzer, B., Cola, M., Griggs, E., 1995. Chemoarchitectonics and corticocortical terminations within the superior temporal sulcus of the rhesus monkey: evidence for subdivisions of superior temporal polysensory cortex. *J. Comp. Neurol.* 360, 513–535.
- de Lima, A.D., Voigt, T., Morrison, J.H., 1990. Morphology of the cells within the inferior temporal gyrus that project to the prefrontal cortex in the macaque monkey. *J. Comp. Neurol.* 296, 159–172.
- DeFelipe, J., Fariñas, I., 1992. The pyramidal neuron of the cerebral cortex: morphological and chemical characteristics of the synaptic inputs. *Prog. Neurobiol.* 39, 563–607.
- Duan, H., He, Y., Wicinski, B., Morrison, J.H., Hof, P.R., 2000. Age-related dendrite and spine changes in corticocortically projecting neurons in macaque monkeys. *Soc. Neurosci. Abstr.* 26, 1237.
- Elston, G.N., 2000. Pyramidal cells of the frontal lobe: all the more spinous to think with. *J. Neurosci.* 20, RC95.
- Elston, G.N., Benavides-Piccione, R., DeFelipe, J., 2001. The pyramidal cell in cognition: a comparative study in human and monkey. *J. Neurosci.* 21, RC163.
- Elston, G.N., Rosa, M.G., 1997. The occipitoparietal pathway of the macaque monkey: comparison of pyramidal cell morphology in layer III of functionally related cortical visual areas. *Cereb. Cortex* 7, 432–452.
- Elston, G.N., Rosa, M.G., 1998. Morphological variation of layer III pyramidal neurones in the occipitotemporal pathway of the macaque monkey visual cortex. *Cereb. Cortex* 8, 278–294.
- Elston, G.N., Rosa, M.G., Calford, M.B., 1996. Comparison of dendritic fields of layer III pyramidal neurons in striate and extrastriate visual areas of the marmoset: a Lucifer Yellow intracellular injection. *Cereb. Cortex* 6, 807–813.
- Elston, G.N., Tweedale, R., Rosa, M.G., 1999a. Cellular heterogeneity in cerebral cortex: a study of the morphology of pyramidal neurones in visual areas of the marmoset monkey. *J. Comp. Neurol.* 415, 33–51.
- Elston, G.N., Tweedale, R., Rosa, M.G., 1999b. Cortical integration in the visual system of the macaque monkey: large-scale morphological differences in the pyramidal neurons in the occipital, parietal and temporal lobes. *Proc. R. Soc. London Ser. B* 266, 1367–1374.
- Elston, G.N., Tweedale, R., Rosa, M.G., 1999c. Supragranular pyramidal neurones in the medial posterior parietal cortex of the macaque monkey: morphological heterogeneity in subdivisions of area 7. *NeuroReport* 10, 1925–1929.
- Goldman-Rakic, P.S., 1988. Topography of cognition: parallel distributed networks in primate association cortex. *Annu. Rev. Neurosci.* 11, 137–156.
- Goldman-Rakic, P.S., 1995. Cellular basis of working memory. *Neuron* 14, 477–485.
- Goldman-Rakic, P.S., 1996. Regional and cellular fractionation of working memory. *Proc. Natl. Acad. Sci. USA* 93, 13473–13480.
- Hallman, L.E., Schofield, B.R., Lin, C.S., 1988. Dendritic morphology and axon collaterals of corticotectal, corticopontine, and callosal neurons in layer V of primary visual cortex of the hooded rat. *J. Comp. Neurol.* 272, 149–160.
- Henry, B.I., Hof, P.R., Rothnie, P., Wearne, S.L., 2002. Fractal analysis of aggregates of non-uniformly sized particles: an application to macaque monkey cortical pyramidal neurons. In: Nowak, M.M. (Ed.), *Emergent Nature: Patterns, Growth and Scaling in the Sciences*. World Scientific, Singapore, pp. 65–75.
- Hof, P.R., Cox, K., Morrison, J.H., 1990. Quantitative analysis of a vulnerable subset of pyramidal neurons in Alzheimer's disease. I. Superior frontal and inferior temporal cortex. *J. Comp. Neurol.* 301, 44–54.
- Hof, P.R., Morrison, J.H., 1990. Quantitative analysis of a vulnerable subset of pyramidal neurons in Alzheimer's disease. II. Primary and secondary visual cortex. *J. Comp. Neurol.* 301, 55–64.
- Hof, P.R., Nimchinsky, E.A., Morrison, J.H., 1995. Neurochemical phenotype of corticocortical connections in the macaque monkey: quantitative analysis of a subset of neurofilament protein-immunoreactive projection neurons in frontal, parietal, temporal, and cingulate cortices. *J. Comp. Neurol.* 362, 109–133.
- Hof, P.R., Nimchinsky, E.A., Young, W.G., Morrison, J.H., 2000. Numbers of Meynert and layer IVB cells in area V1: a stereologic analysis in young and aged macaque monkeys. *J. Comp. Neurol.* 420, 113–126.
- Hof, P.R., Duan, H., Page, T.L., Einstein, M., Wicinski, B., He, Y., Erwin, J.M., Morrison, J.H., 2002. Age-related changes in GluR2 and NMDAR1 glutamate receptor subunit protein immunoreactivity in corticocortically projecting neurons in macaque and patas monkey. *Brain Res.* 928, 175–186.
- Hübener, M., Bolz, J., 1988. Morphology of identified projection neurons in layer 5 of rat visual cortex. *Neurosci. Lett.* 94, 76–81.
- Hübener, M., Schwarz, C., Bolz, J., 1990. Morphological types of projection neurons in layer 5 of cat visual cortex. *J. Comp. Neurol.* 301, 655–674.

- Jacobs, B., Driscoll, L., Schall, M., 1997. Life-span dendritic and spine changes in areas 10 and 18 of human cortex: a quantitative Golgi study. *J. Comp. Neurol.* 386, 661–680.
- Jacobs, B., Schall, M., Prather, M., Kapler, E., Driscoll, L., Baca, S., Jacobs, J., Ford, K., Wainwright, M., Trembl, M., 2001. Regional dendritic and spine variation in human cerebral cortex: a quantitative Golgi study. *Cereb. Cortex* 11, 558–571.
- Jones, E.G., 1984. Laminar distribution of cortical efferent cells. In: Peters, A., Jones, E.G. (Eds.), *Cerebral Cortex*, vol. 1: Cellular Components of the Cerebral Cortex. Plenum Press, New York, pp. 521–554.
- Kasper, E.M., Larkman, A.U., Lübke, J., Blakemore, C., 1994. Pyramidal neurons in layer 5 of the rat visual cortex. I. Correlation among cell morphology, intrinsic electrophysiological properties, and axon targets. *J. Comp. Neurol.* 339, 459–474.
- Katz, L.C., 1987. Local circuitry of identified projection neurons in cat visual cortex brain slices. *J. Neurosci.* 7, 1223–1249.
- Kritzer, M.F., Goldman-Rakic, P.S., 1995. Intrinsic circuit organization of the major layers and sublayers of the dorsolateral prefrontal cortex in the rhesus monkey. *J. Comp. Neurol.* 359, 131–143.
- Levitt, J.B., Lewis, D.A., Yoshioka, T., Lund, J.S., 1993. Topography of pyramidal neuron intrinsic connections in macaque monkey prefrontal cortex (areas 9 and 46). *J. Comp. Neurol.* 338, 360–376.
- Lund, J.S., Yoshioka, T., Levitt, J.B., 1993. Comparison of intrinsic connectivity in different areas of macaque monkey cerebral cortex. *Cereb. Cortex* 3, 148–162.
- Matsubara, J.A., Chase, R., Thejomayen, M., 1996. Comparative morphology of three types of projection-identified pyramidal neurons in the superficial layers of cat visual cortex. *J. Comp. Neurol.* 366, 93–108.
- Melchitzky, D.S., Sesack, S.R., Pucak, M.L., Lewis, D.A., 1998. Synaptic targets of pyramidal neurons providing intrinsic horizontal connections in monkey prefrontal cortex. *J. Comp. Neurol.* 390, 211–224.
- Mesulam, M.M., 1998. From sensation to cognition. *Brain* 121, 1013–1052.
- Miller, E.K., Cohen, J.D., 2001. An integrative theory of prefrontal cortex function. *Annu. Rev. Neurosci.* 24, 167–202.
- Morrison, J.H., 1993. Differential vulnerability, connectivity, and cell typology. *Neurobiol. Aging* 14, 51–54.
- Morrison, J.H., Hof, P.R., 1997. Life and death of neurons in the aging brain. *Science* 278, 412–419.
- Morrison, J.H., Lewis, D.A., Campbell, M.J., Huntley, G.W., Benson, D.L., Bouras, C., 1987. A monoclonal antibody to non-phosphorylated neurofilament protein marks the vulnerable cortical neurons in Alzheimer's disease. *Brain Res.* 416, 331–336.
- Nimchinsky, E.A., Hof, P.R., Young, W.G., Morrison, J.H., 1996. Neurochemical, morphologic, and laminar characterization of cortical projection neurons in the cingulate motor areas of the macaque monkey. *J. Comp. Neurol.* 374, 136–160.
- Nimchinsky, E.A., Sabatini, B.L., Svoboda, K., 2002. Structure and function of dendritic spines. *Annu. Rev. Physiol.* 64, 313–353.
- Page, T.L., Einstein, M., Duan, H., He, Y., Flores, T., Rolshud, D., Erwin, J.M., Wearne, S.L., Morrison, J.H., Hof, P.R., 2002. Morphological alterations in neurons forming corticocortical projections in the neocortex of aged Patas monkeys. *Neurosci. Lett.* 317, 37–41.
- Pucak, M.L., Levitt, J.B., Lund, J.S., Lewis, D.A., 1996. Patterns of intrinsic and associational circuitry in monkey prefrontal cortex. *J. Comp. Neurol.* 376, 614–630.
- Rodriguez, A., Kelliher, K.T., Ehlenberger, D., Henderson, S.C., Einstein, M., Rolshud, D., Duan, H., Morrison, J.H., Wearne, S.L., Hof, P.R., 2001. Implementation of algorithms for high resolution 3-D morphologic analysis of identified cortical neurons: application to age-related alterations. *Soc. Neurosci. Abstr.* 27, 316.9 (<http://www.sfn.org>).
- Rumberger, A., Schmidt, M., Lohmann, H., Hoffmann, K.P., 1998. Correlation of electrophysiology, morphology, and functions in corticotectal and corticopretectal projection neurons in rat visual cortex. *Exp. Brain Res.* 119, 375–390.
- Sholl, D.A., 1953. Dendritic organization of the neurons of the visual and motor cortices of the cat. *J. Anat.* 87, 387–406.
- Sholl, D.A., 1955. The surface area of cortical neurons. *J. Anat.* 89, 571–572.
- Soloway, A.S., Pucak, M.L., Melchitzky, D.S., Lewis, D.A., 2002. Dendritic morphology of callosal and ipsilateral projection neurons in monkey prefrontal cortex. *Neuroscience* 109, 461–471.
- Somogyi, P., Tamas, G., Lujan, R., Buhl, E.H., 1998. Salient features of synaptic organisation in the cerebral cortex. *Brain Res. Rev.* 26, 113–135.
- Trommald, M., Hulleberg, G., 1997. Dimensions and density of dendritic spines from rat dentate granule cells based on reconstructions from serial electron micrographs. *J. Comp. Neurol.* 377, 15–28.
- Uylings, H.B., Ruiz-Marcos, A., van Pelt, J., 1986. The metric analysis of three-dimensional dendritic tree patterns: a methodological review. *J. Neurosci. Methods* 18, 127–151.
- Weinberger, D.R., 1993. A connectionist approach to the prefrontal cortex. *J. Neuropsychiatry Clin. Neurosci.* 5, 241–253.
- Young, W.G., Nimchinsky, E.A., Hof, P.R., Morrison, J.H., Bloom, F.E., 1997. *NeuroZoom Software User Guide and Reference Books*. YBM, San Diego, CA.
- Yuste, R., Tank, D.W., 1996. Dendritic integration in mammalian neurons a century after Cajal. *Neuron* 16, 701–716.

(Accepted 16 April 2002)